

PHYSICAL REVIEW B

CONDENSED MATTER AND MATERIALS PHYSICS

THIRD SERIES, VOLUME 59, NUMBER 19

15 MAY 1999-I

BRIEF REPORTS

*Brief Reports are accounts of completed research which, while meeting the usual **Physical Review B** standards of scientific quality, do not warrant regular articles. A Brief Report may be no longer than four printed pages and must be accompanied by an abstract. The same publication schedule as for regular articles is followed, and page proofs are sent to authors.*

Magnetic destabilization of Ni₇Al

C. Wolverton* and Alex Zunger

National Renewable Energy Laboratory, Golden, Colorado 80401

(Received 25 November 1998)

Previously unknown cubic ordered Ni₇Al and Cu₇Pt compounds have recently been theoretically predicted to be stable phases in the Ni-Al and Cu-Pt systems. While Cu₇Pt was subsequently synthesized and identified, Ni₇Al remains experimentally unobserved. Using first-principles total energy calculations, we reinvestigate the stability of this Ni₇Al compound. We find the stability of this compound to be qualitatively effected by spin polarization, ignored in previous calculations. The effect of ferromagnetism is to stabilize the two-phase mixture of Ni+Ni₃Al relative to the Ni₇Al compound such that the latter is stable in nonmagnetic calculations, but unstable when spin polarization is taken into account. This reversal of relative stabilities of Ni₇Al and Ni+Ni₃Al with magnetism also has a dramatic effect on the calculated Ni₃Al/Ni interfacial energy σ and spin-polarized calculations lead to a positive value of σ , which is in qualitative agreement with values obtained from precipitation experiments. [S0163-1829(99)05319-9]

The Ni-rich portion of the Ni-Al phase diagram^{1,2} has been extensively studied due to the interest in Ni₃Al as a high-temperature alloy and a strengthener in Ni-based superalloys. Although the currently assessed Ni-Al phase diagram^{1,2} contains no ordered phases for composition ranges between that of Ni₃Al and Ni, Lu *et al.*³ predicted the stability of a cubic-ordered Ni₇Al phase (Ca₇Ge-type, space group: $Fm\bar{3}m$, Pearson symbol $cF32$). Because this cubic phase does not have a Strukturbericht notation, these authors denoted this phase “D7,” a notation that we adopt (Fig. 1). The same A_7B structure was previously unknown in the Cu-Pt phase diagram, but was predicted by Lu *et al.*^{3,4} Subsequently, Cu₇Pt was synthesized and identified via x-ray diffraction.⁵ Subsequent to the prediction for Ni₇Al, Chen and Ardell⁶ examined irradiated samples near the Ni₇Al composition for signs of the ordered phase. Irradiated samples were used in hopes of speeding the sluggish kinetics at low temperature, where the compound was predicted to be stable. This technique has been used to produce other hard-to-stabilize compounds with relatively dilute compositions, such as A_8B compounds.⁷ Although the predicted A_7B compound should be clearly observable in Ni-Al (as was the case in Cu₇Pt) due to superlattice peaks at $\frac{1}{2}\langle 111 \rangle$ (which are not present in either Ni₃Al or Ni), no such superlattice peaks were found by Chen and Ardell. Also, diffuse scattering

from a single crystal of the high-temperature Ni-8.9%Al solid solution phase was measured by Schoenfeld *et al.*⁸ These authors examined the measured short-range order present in the solid solution to look for “signatures” of the predicted low-temperature Ni₇Al phase, but no such fingerprints were found.

The previous theoretical prediction of the stability of the D7 phase of Ni₇Al utilized a first-principle total energy approach, although three approximations were used: (i) The energy of the D7 phase was not calculated *directly* from a local-density approximation (LDA) approach, but rather was interpolated using a cluster expansion approach in which LDA energies of several ordered Ni-Al compounds were fit

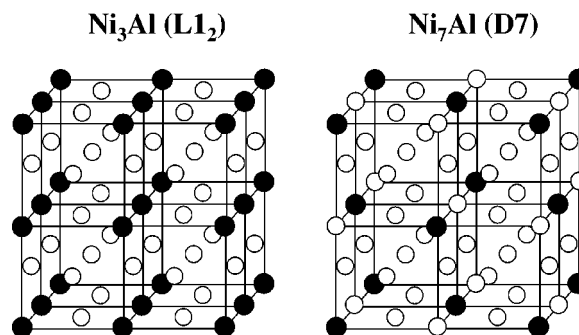


FIG. 1. Structures of Ni₃Al ($L1_2$) and Ni₇Al ($D7$) phases.

to an Ising-like model, which was then used to predict the energies of other phases not calculated (such as $D7$). (ii) The previous approach for Ni-Al (but not Cu-Pt) (Ref. 3) utilized LDA energies based on the method of linear muffin-tin orbitals within the atomic sphere approximation (LMTO-ASA) rather than a full-potential approach. (iii) Nonmagnetic calculations were employed. Due to the absence of experimental evidence for this phase in Ni-Al and the approximations involved in the previous prediction, we decided to reinvestigate this problem theoretically. Thus, we wish to re-examine the stability of the cubic Ni_7Al phase without using any of the approximations of the previous study. Hence, we perform this study using: (i) direct LDA total energies (i.e., not a cluster expansion), (ii) full-potential linearized augmented plane-wave (LAPW) calculations⁹ (rather than LMTO-ASA), and (iii) spin-polarized calculations (both with and without spin-orbit interaction).

In this paper, we do not perform a complete ground-state search, i.e., find the phase has the lowest energy of any compound at that composition (including two-phase mixtures of compounds at other compositions). Instead, we concentrate on a much simpler problem of directly studying the energetics of three *given* phases: Ni, Ni_3Al , and Ni_7Al . Specifically, we will examine the relative stability of cubic Ni_7Al ($D7$) and $\text{Ni}+\text{Ni}_3\text{Al}$ ($L1_2$):

$$\delta E = \frac{1}{8} \{E(\text{Ni}_7\text{Al}, D7) - [4E(\text{Ni}, \text{fcc}) + E(\text{Ni}_3\text{Al}, L1_2)]\}. \quad (1)$$

Thus, δE gives the energy (per atom) by which $D7$ differs from a two-phase mixture of Ni and Ni_3Al . $\delta E < 0$ is a necessary (but not sufficient) condition for the stability of the $D7$ phase. However, if $\delta E > 0$ then the $D7$ phase cannot be the ground state.

We find that (i) a direct approach (rather than cluster expansion) or (ii) a full potential LAPW approach (rather than LMTO-ASA) both give $\delta E < 0$, indicating the stability of the $D7$ phase, in agreement with the findings of Lu *et al.* However, (iii) allowing for ferromagnetic spin polarization leads to $\delta E > 0$. Specifically, spin polarization lowers the energy of Ni significantly more than either Ni_3Al or Ni_7Al . Thus, magnetic interactions destabilize Ni_7Al preventing it from being a ground state. (Such magnetic interactions are not present in Cu₇Pt since Cu is not magnetic.) Finally, the $D7$ phase is simply a short-period [111] superlattice between Ni and Ni_3Al , and therefore the energy δE is related to the Ni/ Ni_3Al [111] interfacial energy, $\sigma(\text{Ni}/\text{Ni}_3\text{Al}; [111])$. We find that the reversal of sign of δE upon spin polarization also leads to a reversal of the calculated sign of the interfacial energy, and brings the calculated value into qualitative agreement with experimental values.

We have performed LAPW calculations in both nonmagnetic and ferromagnetic spin configurations. We used the exchange correlation of Ceperley and Alder,¹⁰ as parametrized by Perdew and Zunger.¹¹ Also, to check the sensitivity of the results to the specific functional, some nonmagnetic calculations were also performed with the Wigner exchange correlation.¹² The muffin-tin radii are chosen to be 2.2 a.u. for Ni and 2.4 a.u. for Al. A basis set corresponding to an energy cutoff of 16.7 Ry ($RK_{\text{max}}=9.0$) was used. Brillouin-zone integrations are performed using the equivalent \mathbf{k} -point sampling method.¹³ We used 60, 20, and 10 \mathbf{k} points in the

irreducible zone for the Ni (fcc), Ni_3Al ($L1_2$), and Ni_7Al ($D7$) structures, respectively, with each set mapping onto to same 60 special \mathbf{k} points¹⁴ for the fcc structure. This mapping guarantees that the total energy per atom of an elemental metal calculated either with the fcc unit cell or with a larger cell ($L1_2$ or $D7$) are identical. All total energies are optimized with respect only to volume as the phases considered are all cubic with no cell-internal degrees of freedom.

The calculated energetics δE (meV/atom) [Eq. (2)] for Ni_7Al are

$$\begin{aligned} \delta E = & -9.8 \text{ Nonmagnetic} \\ & + 12.8 \text{ Ferromagnetic.} \end{aligned} \quad (2)$$

We next discuss our results.

(1) *Nonmagnetic Calculations*: The energy of $D7$ is below that of a mixture of Ni+ Ni_3Al , i.e., $\delta E_{NM} < 0$. Thus, $D7$ is stable with respect to a two-phase mixture of nonmagnetic Ni and Ni_3Al . This nonmagnetic result is in line with the prediction of Lu *et al.*³ implying that two of the approximations in their calculation [(i) the use of a cluster expansion rather than direct LDA and (ii) the use of the atomic sphere approximation] do not qualitatively change the stability of the Ni_7Al phase. Also, the results in Eq. (2) are given for the Ceperley-Alder exchange correlation, we have also calculated these energetics with the Wigner functional, and we also find $\delta E_{NM} < 0$. It is interesting to note that within a nearest-neighbor-only Ising-like alloy description, $\delta E = 0$, thus, the $D7$ structure is exactly degenerate with a two-phase mixture of $L1_2$ and fcc. It is not until first- through fourth-neighbor pairs are considered that the $D7$ structure can become a ground state of the fcc ordering problem.¹⁵

(2) *Ferromagnetic Spin Arrangements*: Despite the fact that ferromagnetism does not significantly lower the energy of Ni_3Al or Ni_7Al , both these structures are predicted to be weakly ferromagnetic. The energetics change qualitatively from $\delta E_{NM} < 0$ to $\delta E_{FM} > 0$. The energetic effect of spin polarization is to lower the energy of Ni much more than that of Ni_7Al or Ni_3Al and hence, to lower the energy of the two-phase mixture Ni+ Ni_3Al below that of Ni_7Al . The same trend in *relative* stabilization energies is seen in the Ni magnetic moment being 0.59, 0.20, and 0.16/0.26 μ_B /atom in Ni, Ni_3Al , and the two inequivalent sites in Ni_7Al , respectively.¹⁶ Thus, *magnetism stabilizes Ni_7Al by less than Ni+ Ni_3Al , so that the $D7$ structure is not stable, and thus these calculations are consistent with the lack of observation of this structure.* Inclusion of the spin-orbit interaction in a second variational procedure¹⁷ does not change the results for the destabilization of the Ni_7Al structure. The spin-orbit interaction reduces the energy of Ni, Ni_3Al , and Ni_7Al all by similar amounts, and leaves the value of δE virtually unchanged. We have performed similar calculations for Ni-Si and Ni-Ti and interestingly, Ni_7Si is also stable nonmagnetically and destabilized by magnetism ($\delta E_{NM} = -0.8$ and $\delta E_{FM} = +20.8$), but Ni_7Ti is not stable either with or without magnetism ($\delta E_{NM} = +22.9$ and $\delta E_{FM} = +48.6$).

The values calculated in Eq. (2) are within the *local* spin-density approximation (LSDA). Ni is difficult to describe accurately within the LSDA, as evidenced by the famous discrepancies that exist between calculated and experimental

values of exchange splitting and bandwidth.^{18–21} The calculated magnetic moment in pure Ni ($0.59 \mu_B/\text{atom}$) is in good agreement with the observed value ($0.61 \mu_B/\text{atom}$); however, as in previous calculations,^{22–25} the calculated magnetic moment of Ni in the Ni₃Al compound ($0.20 \mu_B/\text{atom}$) is higher than the experimental value $0.08 \mu_B/\text{atom}$.²⁶

(3) *Implication of Magnetism on Superlattice Stability:* The destabilization of the Ni₇Al structure with spin polarization also has interesting consequences on the calculated Ni/Ni₃Al interfacial energies. The energy of a coherent $A_p B_p$ superlattice between materials A and B can be separated into two components:²⁷ (a) *Coherency Strain:* the strain energy required to maintain coherency between the (lattice mismatched) materials A and B , and (b) *Interfacial Energy:* the energy associated with the interactions between materials at the A/B interface(s). To define these terms, it is useful to first consider the infinite period superlattice limit $p \rightarrow \infty$, for a superlattice along an orientation \hat{G} with lattice constants a_{\parallel} and a_{\perp} parallel and perpendicular to \hat{G} , respectively. In this infinite-period case, A/B interfacial interactions (which scale as the *area* of the interface) contribute a negligible amount to the superlattice formation energy δE_{SL} (which scales as the *volume* of the superlattice)

$$\begin{aligned} \delta E_{\text{SL}}(p \rightarrow \infty, \hat{G}) &\equiv \delta E_{\text{CS}}(\hat{G}) \\ &= \min_{a_{\perp}} \left[\frac{1}{2} \delta E_A^{\text{epi}}(a_{\perp}, a_{\parallel}^A, \hat{G}) \right. \\ &\quad \left. + \frac{1}{2} \delta E_B^{\text{epi}}(a_{\perp}, a_{\parallel}^B, \hat{G}) \right], \end{aligned} \quad (3)$$

where δE_{SL} is the energy of the superlattice relative to equivalent amounts of A and B in their equilibrium bulk geometries. In Eq. (3), the materials A and B are deformed in an ‘‘epitaxial’’ geometry: Both materials are brought to a common lattice constant a_{\perp} perpendicular to \hat{G} , and the energy of each material is individually minimized with respect to the lattice constant a_{\parallel} parallel to \hat{G} . The epitaxial energies δE_{epi} are the energies of A and B in these epitaxial geometries relative to their equilibrium bulk energy. Summing together these ‘‘epitaxial’’ energies and subsequently minimizing with respect to the common lattice constant gives the coherency strain energy of Eq. (3). For finite-period superlattices, the energy (per atom) is determined not only by the coherency strain energy, but also by the interfacial energy σ , which is proportional to the number of interfaces per atom per unit cell, $2/2p$. We define this interfacial energy as

$$\delta E_{\text{SL}}(p, \hat{G}) - \delta E_{\text{SL}}(p \rightarrow \infty, \hat{G}) \equiv \frac{\sigma(p, \hat{G})}{p}. \quad (4)$$

Combining Eqs. (3) and (4), we see the decomposition of the superlattice energy (for *any* period) into strain and interfacial components

$$\delta E_{\text{SL}}(p, \hat{G}) = \frac{\sigma(p, \hat{G})}{p} + \delta E_{\text{CS}}(\hat{G}). \quad (5)$$

The $D7$ Ni₇Al structure can be considered a very short-period ($p=1$) superlattice between $A=\text{Ni}_3\text{Al}$ and $B=\text{Ni}$

along the $\hat{G}=[111]$ direction. Thus, the energy of Ni₇Al relative to Ni₃Al and Ni in Eq. (2) gives us $\delta E_{\text{SL}}(p=1, [111])$. The coherency strain of Eq. (3) is calculated by epitaxially deforming the ‘‘constituents’’ of the superlattice, Ni₃Al ($L1_2$) and Ni, along the $[111]$ direction, obtaining $\delta E_{\text{CS}}(p=1, [111])$. We then obtain the Ni₃Al/Ni interfacial energy $\sigma(1, [111])$ from Eq. (4).²⁹

The calculated coherency strain energies (meV/atom) are

$$\begin{aligned} \delta E_{\text{CS}}([111]) &= +2.1 \text{ Nonmagnetic} \\ &\quad + 2.1 \text{ Ferromagnetic} \end{aligned} \quad (6)$$

and the resulting Ni₃Al/Ni interfacial energies (mJ/m²) are

$$\begin{aligned} \sigma(1, [111]) &= -37 \text{ Nonmagnetic} \\ &\quad + 33 \text{ Ferromagnetic.} \end{aligned} \quad (7)$$

Of course, the reversal in stability of the Ni₇Al phase with spin polarization implies that the superlattice energy δE_{SL} of Eq. (2) changes upon inclusion of ferromagnetism. However, the fact that $\delta E_{\text{CS}} < |\delta E_{\text{SL}}|$ also implies that *the calculated* Ni₃Al/Ni interfacial energy σ changes from negative to positive with spin polarization. The ferromagnetic results²⁹ are in qualitative agreement with experimental results extracted from Ostwald ripening measurements of Ni₃Al precipitation in Ni-rich alloys: $+8.1 \pm 0.2 \text{ mJ/m}^2$.²⁸ Although the calculated result is much larger than the experimental value, we consider this agreement to be reasonable when one considers that the calculation of the interfacial energy is approximate for several reasons: The zero-temperature calculation is for a very short-period superlattice, the interfacial energy is calculated between stoichiometric, ferromagnetic Ni and Ni₃Al (whereas in the experiment it is at high temperature between Ni₃Al and a Ni-rich solid solution³⁰), and the calculation is for a (111) interface (whereas the data extracted from precipitation kinetics involves an aging schedule in which the precipitates evolve from a spherical to a more cuboidal shape, and thus can only be considered an ‘‘average’’ value). The change in sign of the interfacial energy with spin polarization is also consistent with the calculation of Price and Cooper²⁵ who calculated the (100) Ni₃Al/Ni interfacial energies and also found negative (positive) interfacial energies in their nonmagnetic (ferromagnetic) calculations. However, these authors found even larger interfacial energies ($63\text{--}88 \text{ mJ/m}^2$) than our results.

In sum, we have reinvestigated the stability of the predicted Ni₇Al phase using state-of-the-art first-principles tools based on the local spin-density approximation. We find that spin polarization qualitatively changes the stability of this phase with respect to decomposition into Ni₃Al+Ni, and that the ferromagnetic calculations demonstrate that the Ni₇Al phase is *not stable*. Furthermore, this qualitative shift of energetics upon spin polarization also dramatically affects the Ni₃Al/Ni interfacial energies, bringing them into qualitative agreement with values deduced from precipitation experiments.

The work at NREL was supported by the Office of Energy Research (OER) [Division of Materials Science of the Office of Basic Energy Sciences (BES)], U. S. Department of Energy, under Contract No. DE-AC36-83CH10093.

- *Present address: Ford Motor Company, MD 3028/SRL, P.O. Box 2053, Dearborn, MI 48121-2053.
- ¹T. B. Massalski, *Binary Alloy Phase Diagrams* (ASM International, Metals Park, OH, 1986).
- ²R. Hultgren, R. D. Desai, D. T. Hawkins, M. Gleiser, and K. K. Kelley, *Selected Values of the Thermodynamic Properties of Binary Alloys* (American Society for Metals, Metals Park, OH, 1973).
- ³Z. W. Lu, S.-H. Wei, A. Zunger, S. Frota-Pessoa, and L. G. Ferreira, *Phys. Rev. B* **44**, 512 (1991).
- ⁴Z. W. Lu, S.-H. Wei, and A. Zunger, *Phys. Rev. Lett.* **66**, 1753 (1991).
- ⁵S. Takizawa, *J. Phys. Soc. Jpn.* **65**, 2178 (1996).
- ⁶F. Chen and A. Ardell (private communication).
- ⁷J. Cheng and A. J. Ardell, *Acta Metall.* **37**, 1891 (1989); J. Cheng, M. S. Mostafa, and A. J. Ardell, *J. Less-Common Met.* **143**, 251 (1988); J. Cheng and A. J. Ardell, *ibid.* **141**, 45 (1988).
- ⁸B. Schonfeld, L. Reinhard, G. Kostorz, and W. Buhner, *Acta Mater.* **45**, 5187 (1997).
- ⁹D. J. Singh, *Planewaves, Pseudopotentials, and the LAPW Method* (Kluwer, Boston, 1994).
- ¹⁰S.-H. Wei and H. Krakauer, *Phys. Rev. Lett.* **55**, 1200 (1985); D. M. Ceperley and B. J. Alder, *Phys. Rev. Lett.* **45**, 566 (1980).
- ¹¹J. P. Perdew and A. Zunger, *Phys. Rev. B* **23**, 5048 (1981).
- ¹²E. Wigner, *Phys. Rev.* **46**, 1002 (1934).
- ¹³S. Froyen, *Phys. Rev. B* **39**, 3168 (1989).
- ¹⁴H. J. Monkhorst and J. D. Pack, *Phys. Rev. B* **13**, 5188 (1976).
- ¹⁵J. Kanamori and Y. Kakehashi, *J. Phys. Colloq. (Paris)* **38**, C7-274 (1977).
- ¹⁶In the Ni₇Al structure, there are two symmetry-distinct Ni-sites, Ni₁ and Ni₂. Interestingly, the Ni₁ site, which is surrounded entirely by 12 Ni atoms in the first-neighbor shell has a *smaller* magnetic moment (0.16) than the site Ni₂, which is surrounded by 10 Ni + 2 Al nearest neighbors ($\mu = 0.26$). This result can be explained by the second-neighbor environments, which are extremely different for these two types of atoms: Ni₁ is surrounded by 6 Al atoms (thereby producing a lower magnetic moment) whereas Ni₂ is surrounded by 6 Ni atoms (thereby pushing the magnetic moment up towards that of pure Ni). These results imply that magnetic moments in Ni-Al are not simply related to the nearest-neighbor environments surrounding each atom, but rather are more likely related to a longer-ranged function of each atom's local environment. Previous LDA calculations have also examined the correlation between magnetic moment and local environment [Y. Wang *et al.*, in *Materials Theory, Simulations, and Parallel Algorithms* (Ref. 25), pp. 585–590; S.-H. Wei and A. Zunger, *Phys. Rev. B* **48**, 6111 (1993)].
- ¹⁷A. H. MacDonald, W. E. Pickett, and D. D. Koelling, *J. Phys. C* **13**, 2675 (1980); W. E. Pickett, A. J. Freeman, and D. D. Koelling, *Phys. Rev. B* **23**, 1266 (1981).
- ¹⁸W. Eberhardt and E. W. Plummer, *Phys. Rev. B* **21**, 3245 (1980).
- ¹⁹D. E. Eastman, F. J. Himpsel, and J. A. Knapp, *Phys. Rev. Lett.* **40**, 1514 (1978).
- ²⁰F. J. Himpsel, J. A. Knapp, and D. E. Eastman, *Phys. Rev. B* **19**, 2919 (1979).
- ²¹S. Hufner, G. K. Wertheim, N. V. Smith, and M. M. Tram, *Solid State Commun.* **11**, 323 (1972).
- ²²B. I. Min, A. J. Freeman, and H. J. F. Jansen, *Phys. Rev. B* **37**, 6757 (1988).
- ²³J.-H. Xu, B. I. Min, A. J. Freeman, and T. Oguchi, *Phys. Rev. B* **41**, 5010 (1990).
- ²⁴V. L. Moruzzi and P. M. Marcus, *Phys. Rev. B* **42**, 5539 (1990).
- ²⁵D. L. Price and B. R. Cooper, in *Materials Theory, Simulations, and Parallel Algorithms*, edited by E. Kaxiras, J. Joannopoulos, P. Vashishta, and R. Kalia, MRS Symposium Proceedings No. 408 (Materials Research Society, Pittsburgh, 1996), p. 463.
- ²⁶F. R. de Boer, C. J. Schinkel, J. Biesterbos, and S. Proost, *J. Appl. Phys.* **40**, 1049 (1969).
- ²⁷V. Ozolins, C. Wolverton, and A. Zunger, *Phys. Rev. B* **57**, 4816 (1998).
- ²⁸A. J. Ardell, *Interface Sci.* **3**, 119 (1995).
- ²⁹The coherency strain of Eq. (3) is defined in the long-period superlattice limit; however, there is a slight ambiguity about how the strain should be evaluated for a short-period superlattice. We have used the long-period limit of the coherency strain in evaluating the interfacial energies via Eq. (5), however one could also obtain the strain of a short-period superlattice by taking the energy of Ni₃Al and Ni *strained to the geometry of the superlattice*. Since our superlattice is the cubic *D7* structure with no distortions, this alternate approach amounts to simply looking at the hydrostatic, not epitaxial, deformation of the endpoints. This hydrostatic strain is larger than the long-period epitaxial strain and would result in slightly lower interfacial energies if used in Eq. (5).
- ³⁰Recent first-principles calculations [M. Sluiter and Y. Kawazoe, *Phys. Rev. B* **54**, 10 381 (1996); M. Asta, S. M. Foiles, and A. A. Quong, *ibid.* **57**, 11 265 (1998)] have demonstrated that configurational entropy can significantly reduce σ relative to its zero-*T* value.